



25 presence or absence of Al_2O_3 seed aerosols in a 2 m^3 smog chamber. The
26 presence of SO_2 increased new particle formation and particle growth
27 significantly, regardless of whether NH_3 was present or not. Sulfate,
28 organic aerosol, nitrate and ammonium were all found to increase linearly
29 with increasing SO_2 concentrations. The increases in these four species
30 were more obvious under NH_3 -rich conditions, and the generation of nitrate,
31 ammonium and organic aerosol increased more significantly than sulfate
32 with respect to SO_2 concentration, while sulfate was the most sensitive
33 species under NH_3 -poor conditions. The synergistic effects between SO_2
34 and NH_3 in the heterogeneous process contributed greatly to secondary
35 aerosol formation. Specifically, the generation of NH_4NO_3 was found to be
36 highly dependent on the surface area concentration of suspended particles,
37 and increased most significantly among the four species with respect to
38 SO_2 concentration under ammonia-rich conditions. Meanwhile, the
39 absorbed NH_3 might provide a liquid surface layer for the absorption and
40 subsequent reaction of SO_2 and organic products, and therefore, enhance
41 sulfate and secondary organic aerosol (SOA) formation. This effect mainly
42 occurred in the heterogeneous process and resulted in a significantly higher
43 growth rate of seed aerosols compared to that without NH_3 . By applying
44 positive matrix factorization (PMF) analysis to the AMS data, two factors
45 were identified for the generated SOA. One factor, assigned to less-
46 oxidized organic aerosol and some oligomers, increased with increasing
47 SO_2 under NH_3 -poor conditions, mainly due to the well-known acid
48 catalytic effect of the acid products on SOA formation in the heterogeneous



49 process. The other factor, assigned to the highly oxidized organic
50 component and some nitrogen-containing organics (NOC), increased with
51 SO₂ under a NH₃-rich environment, with NOC (organonitrates and NOC
52 with reduced N) contributing most of the increase.

53 **Introduction**

54 With the recent rapid economic development and urbanization, the
55 associated emissions from coal combustion, motor vehicle exhaust and
56 various industrial emissions have led to highly complex air pollution in
57 China. Besides the high concentrations of fine particles (PM_{2.5}), high
58 concentrations of NO_x, SO₂, NH₃, and volatile organic compounds (VOCs)
59 were observed in haze pollution episodes (Liu et al., 2013; Ye et al., 2011;
60 Zou et al., 2015; Wang et al., 2015). For example, the SO₂ concentration in
61 Jinan, a city in North China, can be as high as 43 ppb in the winter season
62 (Wang et al., 2015). The high concentrations of precursors resulted in high
63 concentrations of secondary inorganic and organic species in PM_{2.5} during
64 haze formation (Yang et al., 2011; Zhao et al., 2013; Dan et al., 2004; Duan
65 et al., 2005; Wang et al., 2012). There has been no extensive measurement
66 of NH₃ in China despite its extensive emission and increasing trend (Fu et
67 al., 2015). A few studies reported high concentrations of NH₃ (maximum
68 concentration higher than 100 ppb) in the North China Plain (Meng et al.,
69 2015; Wen et al., 2015) and many observation data indicated NH₃-rich
70 conditions for secondary aerosol formation, and strong correlations
71 between peak levels of fine particles and large increases in NH₃



72 concentrations in China (Ye et al., 2011; Liu et al., 2015a). Under this
73 complex situation, studying the synergistic effects of SO₂ and NH₃ among
74 pollutants in secondary aerosol formation is crucial in order to understand
75 the formation mechanism of heavy haze pollution.

76 Interactions between inorganic pollutants in secondary aerosol
77 formation have been investigated extensively. For example, NO₂ was found
78 to increase the oxidation of SO₂ in aqueous aerosol suspensions (Tursic and
79 Grgic, 2001) and on a sandstone surface (Bai et al., 2006). The synergistic
80 reaction between SO₂ and NO₂ on mineral oxides was reported (Liu et al.,
81 2012a) and proposed to explain the rapid formation of sulfate during heavy
82 haze days (He et al., 2014). The presence of NH₃ was also found to enhance
83 the conversion of SO₂ to sulfate in aerosol water and on the surface of
84 mineral dust or PM_{2.5} (Tursic et al., 2004; Behera and Sharma, 2011; Yang
85 et al., 2016).

86 Secondary aerosol formation from coexisting inorganic and organic
87 pollutants is far more complicated. There have been a few studies that
88 investigated the effects of SO₂ or NH₃ on secondary organic aerosol (SOA)
89 formation. SO₂ has been found to enhance SOA yield from isoprene (Edney
90 et al., 2005; Kleindienst et al., 2006; Lin et al., 2013), α -pinene
91 (Kleindienst et al., 2006; Jaoui et al., 2008), and anthropogenic precursors
92 (Santiago et al., 2012) due to its acidic aerosol products, which were
93 thought to either take up organic species (Liggio and Li, 2008, 2006) or
94 result in the formation of high molecular weight compounds in acid-
95 catalytic reactions (Liggio et al., 2007; Kleindienst et al., 2006; Santiago



96 et al., 2012). Besides, sulfate esters were also confirmed as major players
97 in SOA formation (Schmitt-Kopplin et al., 2010). The effects of NH_3 on
98 SOA formation are relatively poorly understood. In previous studies,
99 disparate effects of NH_3 on secondary aerosol formation were reported. It
100 was found that the presence of NH_3 increased SOA formation in the
101 reaction of α -pinene or cyclohexene with ozone (Na et al., 2007), but had
102 little effect on SOA mass in isoprene ozonolysis (Na et al., 2007; Lin et al.,
103 2013) and even decreased SOA production from the reaction of styrene and
104 ozone (Na et al., 2006). NH_3 was reported to react with some organic acids
105 and contribute to secondary aerosol formation (Na et al., 2007; Lin et al.,
106 2013), while nucleophilic NH_3 might attack and decompose trioxolane and
107 hydroxyl-substituted esters (Na et al., 2006), and therefore decrease SOA
108 mass. Updyke et al. (2012) studied brown carbon formation via reactions
109 of ammonia with SOA from various precursors and emphasized that aging
110 by NH_3 is not a unique mechanism of SOA browning. It was found that the
111 degree of browning had a positive correlation with the carbonyl products,
112 which may react with NH_3 and generate hemiaminal (Amarnath et al.,
113 1991), while the form of ammonia (NH_3 gas or NH_4^+ ion) had little
114 influence on the browning processes.

115 The effects of SO_2 and NH_3 on SOA formation have rarely been
116 investigated together, while the interactive effects between inorganic and
117 organic species under highly complex pollution conditions remain
118 uncertain. This study investigated secondary aerosol formation in the
119 photooxidation of toluene/ NO_x with varied concentrations of SO_2 under



120 NH₃-poor and NH₃-rich conditions. Some synergetic effects in the
121 heterogeneous process that contributed to both secondary inorganic and
122 organic aerosol formation were explored.

123 **Methods**

124 A series of smog chamber experiments were carried out to simulate
125 secondary aerosol formation in the photooxidation of VOC/NO_x in the
126 presence or absence of SO₂ and/or NH₃. The chamber is a 2 m³ cuboid
127 reactor constructed with 50 μm-thick FEP-Teflon film (Toray Industries,
128 Inc., Japan). The chamber was described in detail in Wu *et al.* (2007). A
129 temperature-controlled enclosure (SEWT-Z-120, Escpec, Japan) provides
130 a constant temperature (30±0.5 °C), and 40 black lights (GE F40T12/BLB,
131 peak intensity at 365 nm, General Electric Company, USA) provide
132 irradiation during the experiments. The hydrocarbon concentration was
133 measured by a gas chromatograph (GC, Beifen SP-3420, Beifen, China)
134 equipped with a DB-5 column (30 m×0.53 mm×1.5 mm, Dikma, USA) and
135 flame ionization detector (FID), while NO_x, SO₂ and O₃ were monitored
136 by an NO_x analyzer (Model 42C, Thermo Environmental Instruments,
137 USA), an SO₂ analyzer (Model 43I, Thermo Environmental Instruments,
138 USA) and an O₃ analyzer (Model 49C, Thermo Environmental Instruments,
139 USA), respectively. A scanning mobility particle sizer (SMPS) (TSI 3936,
140 TSI Incorporated, USA) was used to measure the size distribution of
141 particulate matter (PM) in the chamber, and also employed to estimate the
142 volume and mass concentration. The chemical composition of aerosols was



143 measured by an aerosol chemical speciation monitor (ACSM, Aerodyne
144 Research Incorporated, USA) or high resolution time of flight aerosol mass
145 spectrometer (HR-ToF-AMS, Aerodyne Research Incorporated, USA).
146 ACSM is a simplified version of aerosol mass spectrometry (AMS), with
147 similar principles and structure. Ng *et al.* (2011) presented a detailed
148 introduction to this instrument and found that the measurement results
149 agreed well with the AMS. Wall deposition of particles in the chamber was
150 similarly corrected using a regression equation to describe the dependence
151 of deposition rate on the particle size (Takekawa *et al.*, 2003). Detailed
152 information on this equation was given in our previous studies (Chu *et al.*,
153 2012; Chu *et al.*, 2014).

154 Alumina seed particles were produced on-line via a spray pyrolysis
155 setup, which has been described in detail elsewhere (Liu *et al.*, 2010).
156 Liquid alumisol (AlOOH, Lot No. 2205, Kawaken Fine Chemicals Co.,
157 Ltd., Japan) with an initial concentration of 1.0 wt%, was sprayed to
158 droplets by an atomizer. After that, the droplets were carried through a
159 diffusion dryer and a corundum tube embedded in a tubular furnace with
160 the temperature maintained at 1000 °C to generate alumina particles. The
161 obtained alumina particles were γ -Al₂O₃ as detected by X-ray diffraction
162 measurements, and spherical-shaped according to electron micrograph
163 results. Before being introduced into the chamber, the particles were
164 carried through a neutralizer (TSI 3087, TSI Incorporated, USA). In
165 addition, toluene was injected into a vaporizer and then carried into the
166 chamber by purified air, while NO_x, SO₂ and NH₃ were directly injected



167 into the chamber from standard gas bottles. The concentrations of NH_3
168 were estimated according to the introduced amount of NH_3 and the volume
169 of the reactor.

170 **Results and discussion**

171 **Particle formation and growth in different inorganic gas conditions**

172 The effects of SO_2 and NH_3 on secondary aerosol formation were
173 qualitatively studied first in the photooxidation system of toluene/ NO_x
174 without the presence of a seed aerosol. Experiments were carried out in the
175 absence of SO_2 and NH_3 , in the presence of SO_2 or NH_3 , and coexistence
176 of SO_2 and NH_3 , respectively. Experimental details are listed in Table 1.
177 The letter codes used for the experiments represent a combination of the
178 initial letters of the precursors for each experiment. For example,
179 experiment “ASTN” is an experiment with presence of ammonia gas (A),
180 sulfur dioxide (S), toluene (T) and nitrogen oxides (N). Two experiments
181 (ATN1 and ATN2) were carried out under similar conditions to test the
182 reproducibility of the experiments.

183 Secondary aerosol formation in these photooxidation experiments was
184 measured by the SMPS, and the results are displayed in Fig. 1. Assuming
185 the same aerosol density in these experiments, the presence of either NH_3
186 or SO_2 enhanced secondary aerosol formation markedly. Compared to
187 toluene/ NO_x photooxidation, the secondary aerosol volume concentration
188 rose 1.5 times in the presence of SO_2 , and was more than tripled in the



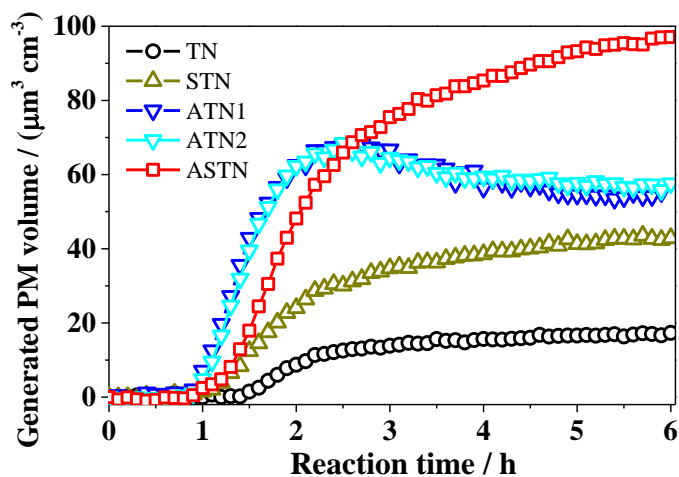
189 presence of the NH_3 . The volume of secondary aerosol showed an obvious
190 peak in the toluene/ NO_x / NH_3 system at about 2.3 hours of photooxidation.
191 With the wall deposition accounted for, the decrease of the volume
192 concentration after that point was unexpected, but could be reproduced
193 (Experiment ATN1 and ATN2). Such a decrease was not observed with
194 coexisting NH_3 and SO_2 , indicating interactions between NH_3 and SO_2 in
195 the photooxidation system. The reason for this phenomenon will be
196 discussed in the following analysis of the chemical composition of the
197 generated particles.

198 Table 1 Initial experimental conditions of toluene/ NO_x photooxidation in the
199 presence or absence of SO_2 and/or NH_3

Experiment	Hydrocarbon	NO	NO_x -NO	SO_2	NH_3^*	RH	T
No.	<i>ppm</i>	<i>ppb</i>	<i>ppb</i>	<i>ppb</i>	<i>ppb</i>	%	K
TN	1.05	54	49	0	0	50	303
STN	1.05	55	50	137	0	50	303
ATN1	1.06	47	48	0	264	50	303
ATN2	0.98	48	54	0	264	50	303
ASTN	1.02	49	53	134	264	50	303

200 *The concentrations of NH_3 were calculated according to the introduced amount of NH_3
201 and the volume of the reactor.

202



203

204

Fig. 1 Secondary aerosol formation in photooxidation of toluene/ NO_x in the

205

presence or absence of NH_3 and/or SO_2 . The letters codes for the experiments

206

indicate the introduced pollutants, i.e. “A” for ammonia, “S” for sulfur dioxide,

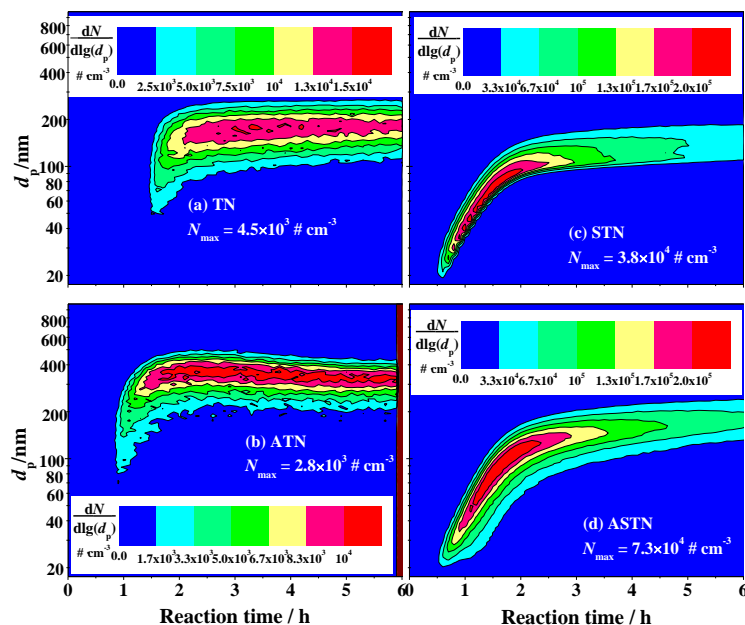
207

“T” for toluene and “N” for nitrogen dioxide. Experimental details are listed in

208

Table 1.

209



210
211 Fig. 2 Size distributions of the suspended particles as a function of time during the
212 reaction in photooxidation of toluene/ NO_x in the presence or absence of NH_3
213 and/or SO_2 . N_{max} shows the maximal particle number concentration during the
214 reaction for each experiment. Experimental details are listed in Table 1.

215 The size distributions of the secondary aerosol in the photooxidation,
216 with a range of 17-1000 nm, were analyzed and are shown in Fig. 2. A
217 significant increase in new particle formation was observed in the presence
218 of SO_2 . The maximal particle number concentrations in experiments ASTN
219 and STN were one order of magnitude higher than those in experiments
220 ATN and TN. The presence of NH_3 also contributed substantially to the
221 particle growth in photooxidation of toluene/ NO_x . Comparing Fig. 2(c) to
222 Fig. 2(a), the total number concentration of particles in experiment ATN
223 was a little lower than that in experiment TN, but the mode diameter of the



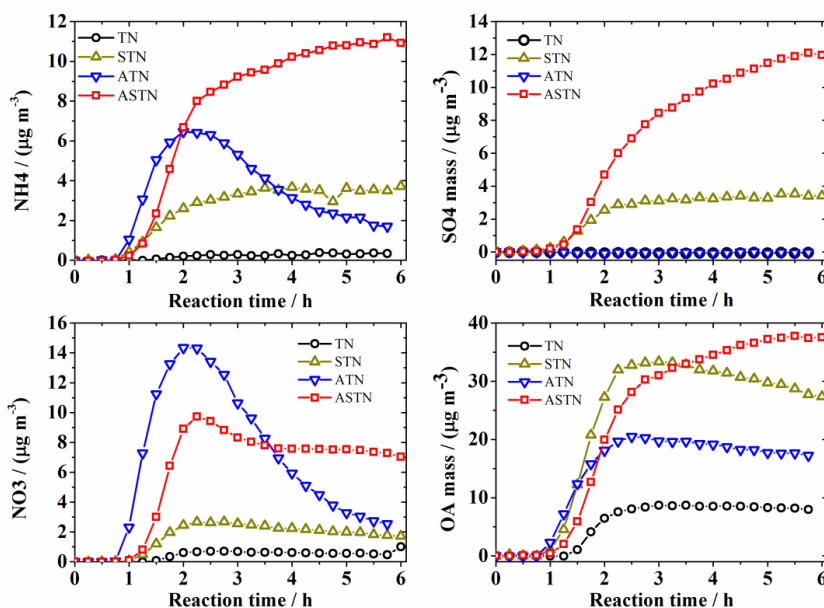
224 particles was much larger.

225 **Secondary inorganic aerosol formation**

226 Some synergetic effects were observed in secondary inorganic aerosol
227 formation besides the generation of ammonium and sulfate from NH_3 and
228 SO_2 . For example, nitrate formation was not only enhanced by NH_3 , due to
229 conversion of nitric acid into ammonia nitrate, but also was markedly
230 affected by SO_2 . The chemical compositions of the generated aerosols in
231 the photooxidation of toluene/ NO_x were analyzed with an ACSM, and their
232 time variations are displayed in Fig. 3. In experiment ATN, the
233 concentrations of ammonium and nitrate decreased after about 2.3 hours of
234 reaction, as shown in Fig. 3, which was consistent with the decreasing trend
235 of particle concentration shown in Fig. 1. The reason for this phenomenon
236 is unknown but we speculate that the generated NH_4NO_3 might partition
237 back into the gas phase as reaction goes on. In Fig. 2, we observed that the
238 particle size was larger in experiment ATN than the other three experiments.
239 The larger diameter resulted in more significant wall deposition, reduced
240 the surface area of the suspended particles, and shifted the partition
241 equilibrium to the gas phase. Adding SO_2 to the system resulted in a lower
242 peak concentration but a higher final concentration of nitrate. In the
243 presence of SO_2 , higher concentrations of sulfate and organic species were
244 generated and mixed with nitrate in the aerosol, which may shift the
245 partition balance of NH_4NO_3 to the aerosol phase. In addition, the presence
246 of organic matter might accelerate the deliquescence of generated



247 inorganic particles (Meyer et al., 2009; Li et al., 2014), and provide moist
248 surfaces for heterogeneous hydrolysis of N_2O_5 , contributing to nitrate
249 formation (Pathak et al., 2009).



250

251 Fig. 3 Time variations of the chemical species in the secondary aerosol generated
252 from the photooxidation of toluene/ NO_x in the presence or absence of NH_3 and
253 SO_2 . Letter codes for experiments indicate the introduced pollutants, i.e. “A” for
254 ammonia, “S” for sulfur dioxide, “T” for toluene and “N” for nitrogen dioxide.

255

Experimental details are listed in Table 1.

256 In Fig. 3, the generation of ammonium salt can be observed in the
257 photooxidation of toluene/ NO_x / SO_2 without introducing NH_3 gas. This
258 indicated there was NH_3 present in the background air in the chamber, and
259 also indicated that the effects of NH_3 on secondary aerosol formation might
260 be underestimated in this study. The background NH_3 was derived from the



261 partitioning of the deposited ammonium sulfate and nitrate on the chamber
262 wall when humid air was introduced (Liu et al., 2015b). Unfortunately, due
263 to the lack of appropriate instrumentation, we were not able to measure the
264 exact concentration of NH_3 in the background air in the chamber. With this
265 in mind, the experiments carried out without introducing NH_3 gas were
266 considered “ NH_3 -poor” experiments in this study, while experiments with
267 the introduction of NH_3 gas were considered “ NH_3 -rich” experiments, in
268 which the concentrations of NH_3 were more than twice the SO_2
269 concentrations and the oxidation products of SO_2 and NO_x were fully
270 neutralized by NH_3 .

271 To further quantify the effect of SO_2 on secondary aerosol formation,
272 different concentrations of SO_2 were introduced under NH_3 -poor and NH_3 -
273 rich conditions. The details of the experimental conditions are shown in
274 Table 2. In these experiments, the concentrations of toluene were reduced
275 compared to the experiments in Table 1, and monodisperse Al_2O_3 seed
276 particles with mode diameter about 100 nm were introduced into the
277 chamber. As shown in Fig. 4, similar to the seed-free experiments, the
278 presence of SO_2 and NH_3 clearly increased secondary aerosol formation in
279 toluene/ NO_x photooxidation in the presence of Al_2O_3 seed aerosols. In the
280 experiments carried out in the presence of Al_2O_3 seed aerosols, the
281 decrease of NH_4NO_3 was not obvious in the experiment carried out in the
282 absence of SO_2 under NH_3 -rich conditions, indicating that generation of
283 NH_4NO_3 was highly dependent on the surface area concentration of the
284 particles, which decreased the partitioning of NH_4NO_3 back to the gas



285 phase, as discussed above.

286 Under both NH_3 -poor and NH_3 -rich conditions, all the detected
287 chemical species in the generated aerosol, including sulfate, organic
288 aerosol, nitrate and ammonium, increased linearly with increasing SO_2
289 concentrations, as shown in Fig. 5. The increase was more significant in a
290 NH_3 -rich environment than that under NH_3 -poor conditions, indicating a
291 synergistic effect of SO_2 and NH_3 on aerosol generation. Among the four
292 chemical species, nitrate generation increased most significantly with
293 respect to SO_2 concentration under NH_3 -rich conditions, followed by
294 ammonium and organic aerosol, while sulfate was the least sensitive
295 species. Under NH_3 -poor conditions, the sensitivity of these species
296 followed a different sequence, in which sulfate > nitrate > organic aerosol >
297 ammonium. A better correlation was found between secondary aerosol
298 formation and particle surface area than that with particle volume, with
299 details introduced in Fig. S1 in the supporting information, indicating an
300 enhancement effect in the heterogeneous process rather than in bulk
301 reactions. The different sequences under NH_3 -rich and NH_3 -poor
302 conditions indicated that the presence of SO_2 and NH_3 not only contributed
303 aerosol surface for partitioning, but also enhanced the heterogeneous
304 process for secondary aerosol formation.

305

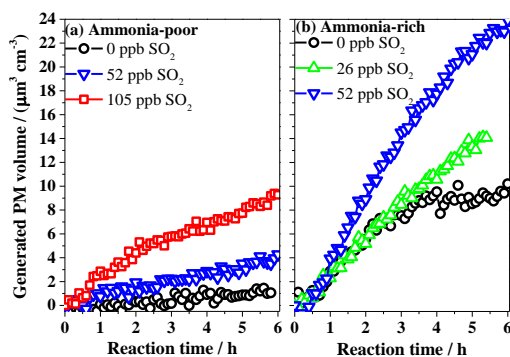
306 Table 2 Experimental conditions of the toluene/ NO_x photooxidation in the presence
307 of different concentrations of SO_2 and Al_2O_3 seed particles under NH_3 -poor and NH_3 -
308 rich conditions



	Toluene ₀	NO ₀	NO _x -NO	SO ₂	Al ₂ O ₃	NH ₃ *	RH	T
	<i>ppb</i>	<i>ppb</i>	<i>ppb</i>	<i>ppb</i>	<i>particle/cm³</i>	<i>ppb</i>	<i>%</i>	<i>K</i>
NH ₃ -poor	188	147	60	0	2400	0	50	303
	200	126	51	52	3100	0	50	303
	188	130	58	105	2100	0	50	303
NH ₃ -rich	197	142	46	0	3300	105	50	303
	220	147	50	26	3300	105	50	303
	207	145	49	52	3200	105	50	303

309 Calculated according to the introduced amount of NH₃ and the volume of the reactor.

310

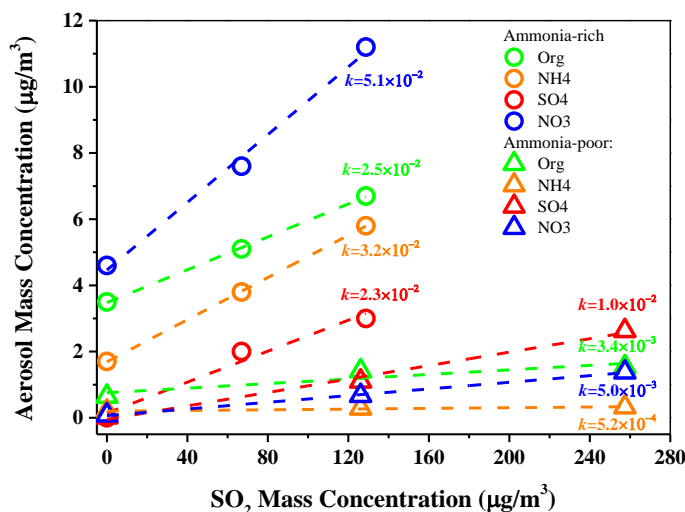


311

312 Fig. 4 Secondary aerosol formation as a function of time with different

313 concentrations of SO₂ in the photooxidation of toluene/NO_x under NH₃-poor (a)

314 and NH₃-rich (b) conditions. Experimental details are listed in Table 1.



315

316 Fig. 5 Formation of nitrate (blue), organic aerosol (green), sulfate (red), and
317 ammonium salt (orange) as functions of SO₂ concentration in the photooxidation
318 of toluene/NO_x under NH₃-rich (circles) or NH₃-poor (triangles) conditions. The *k*
319 values are the slopes of the fitted lines for each species. Experimental details are
320 listed in Table 1.

321

322 Another synergetic effect we found in secondary inorganic aerosol
323 formation was that sulfate formation was enhanced by the presence of NH₃.
324 In both seed-free experiments and experiments in the presence of Al₂O₃
325 seed aerosols, the sulfate mass concentration was more than tripled under
326 NH₃-rich conditions compared to an NH₃-poor environment. This is
327 consistent with previous studies on the reactions of SO₂, NO₂ and NH₃ in
328 smog chambers (Behera and Sharma, 2011) and the heterogeneous reaction
329 between NH₃ and SO₂ on particle surfaces (Yang et al., 2016; Tursic et al.,



330 2004). According to the consumption of toluene, OH concentrations in the
331 photooxidation experiments were estimated to range from 1.6×10^6
332 molecules/cm³ to 2.7×10^6 molecules/cm³. The reaction between these OH
333 radicals and SO₂ contributed 35%-50% of the total SO₂ degradation in
334 NH₃-poor experiments, while this ratio was reduced to 25%-30% in NH₃-
335 rich experiments. This indicated that the heterogeneous process was an
336 important pathway for inorganic aerosol formation in the photooxidation
337 system, and the heterogeneous process was enhanced by the presence of
338 NH₃. This result is consistent with the finding that failure to include the
339 heterogeneous process in the model caused an underestimation of SO₂
340 decay in the chamber (Santiago et al., 2012). According to previous studies,
341 NH₃ might provide surface Lewis basicity and liquid surface layers for SO₂
342 absorption and subsequent oxidation, and therefore, enhance sulfate
343 formation (Yang et al., 2016; Tursic et al., 2004).

344 **Secondary organic aerosol formation**

345 The presence of NH₃ and SO₂ caused significant formation of
346 secondary inorganic aerosol, and meanwhile, enhanced SOA formation. In
347 previous studies, Kleindienst et al. (2006) found that the presence of SO₂
348 did not disturb the dynamic reaction system of α -pinene or isoprene in the
349 presence of NO_x. In the present study, no obvious difference was found in
350 the OH concentration in experiments with different concentrations of SO₂
351 and NH₃. Therefore, it could be also assumed that the presence of SO₂ and
352 NH₃ in this study did not significantly impact the gas phase oxidation of



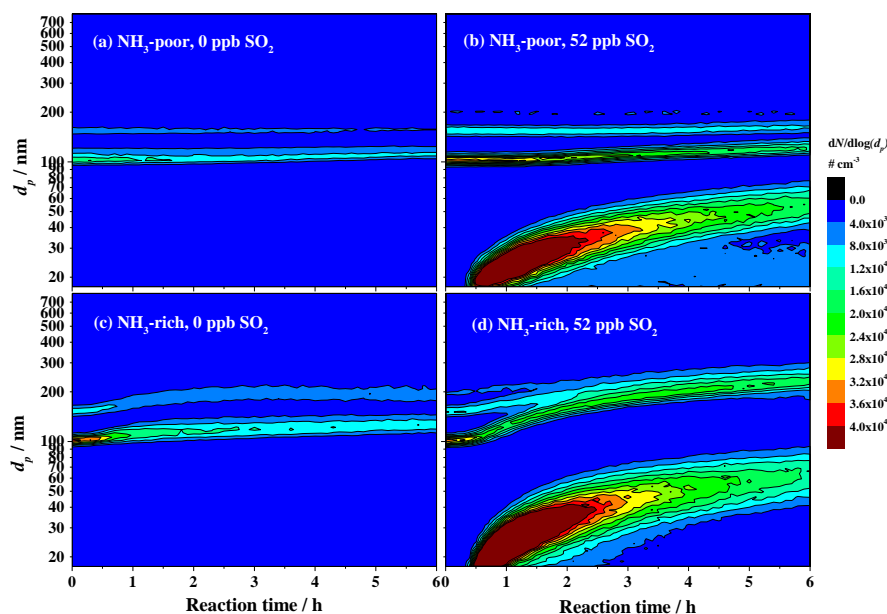
353 hydrocarbons and mainly played a role in the aerosol phase.

354 The presence of NH_3 markedly increased aerosol formation in the
355 photooxidation of toluene/ NO_x . In the seed-free toluene/ NO_x
356 photooxidation experiments, the presence of NH_3 caused similar additional
357 amounts of organic aerosol mass and resulted in increases of 116% and 36%
358 in the absence or presence of SO_2 , respectively. In the experiments carried
359 out in the presence of Al_2O_3 seed aerosols, the increase caused by NH_3 was
360 more significant, with the organic aerosol quantity increasing by a factor
361 of four to five. NH_3 may react with the ring opening oxycarboxylic acids
362 from toluene (Jang and Kamens, 2001), resulting in products with lower
363 volatility. The presence of NH_3 might also change the surface properties of
364 the aerosol and enhance heterogeneous oxidation of organic products. As
365 mentioned earlier in this study, there was NH_3 present in the background
366 air in the chamber, so the effects of NH_3 on secondary aerosol formation
367 might be underestimated in this study. Detecting the concentration of NH_3
368 gas as a function of time and quantifying the effects of NH_3 on secondary
369 aerosol are meaningful, and are expected to be studied in the future.

370 The enhancing effect of NH_3 on secondary aerosol formation in toluene
371 photooxidation was further attributed to its influence in heterogeneous
372 reactions. In the presence of Al_2O_3 seed particles, no obvious new particle
373 formation was detected in experiments without SO_2 , as shown in Fig. 6(a)
374 and Fig. 6(c). The presence of NH_3 caused a more noticeable particle
375 growth of the Al_2O_3 seed particles. The increase mainly took place after
376 0.5 hours of irradiation, and lasted for about an hour, with an average



377 diameter growth of about 12 nm. In the two experiments carried out in the
378 presence of 52 ppb SO₂ in Fig. 7(b) and Fig. 7(d), significant but similar
379 new particle formation occurred. The maximum particle number
380 concentrations detected by the SMPS were about 33000 particle/cm³ and
381 34000 particle/cm³ under NH₃-poor and NH₃-rich conditions, respectively.
382 However, the growth of the seed aerosol in these two experiments was
383 quite different. Under an NH₃-poor condition, the mode diameter of the
384 seed aerosols grew from 100 nm to about 130 nm, while under an NH-rich
385 condition it grew to about 220 nm. These results indicated that elevated
386 NH₃ concentrations mainly affected secondary aerosol formation in the
387 heterogeneous process.



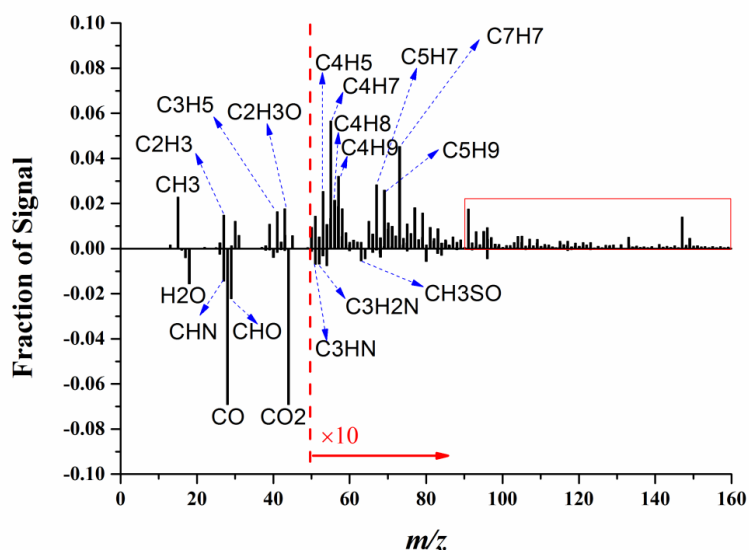
388
389 Fig. 6 Size distributions of the suspended particles as a function of time during the
390 reaction in photooxidation of toluene/NO_x in the presence of Al₂O₃ seed particles.



391 Experimental details are listed in Table 1.

392

393 The chemical properties of the generated SOA under different
394 conditions of NH_3 and SO_2 were compared by applying PMF analysis to
395 the AMS data. Two factors were identified from the analysis, with average
396 elemental composition of $\text{CH}_{0.82}\text{O}_{0.75}\text{N}_{0.051}\text{S}_{0.0014}$ for Factor 1 and
397 $\text{CH}_{1.05}\text{O}_{0.55}\text{N}_{0.039}\text{S}_{0.0017}$ for Factor 2. The difference mass spectra between
398 the two factors are shown in Fig. 7. The abundance of C_xH_y fragments was
399 higher in Factor 2 than Factor 1, while oxygen and nitrogen content in
400 Factor 1 were higher than Factor 2. Meanwhile, as indicated in the red box
401 in Fig. 7, fragments with high m/z were more abundant in Factor 2. Thus
402 we assigned Factor 1 to the highly oxidized organic component and some
403 nitrogenous organic compounds, while Factor 2 was assigned to less-
404 oxidized organic aerosol and some oligomers.



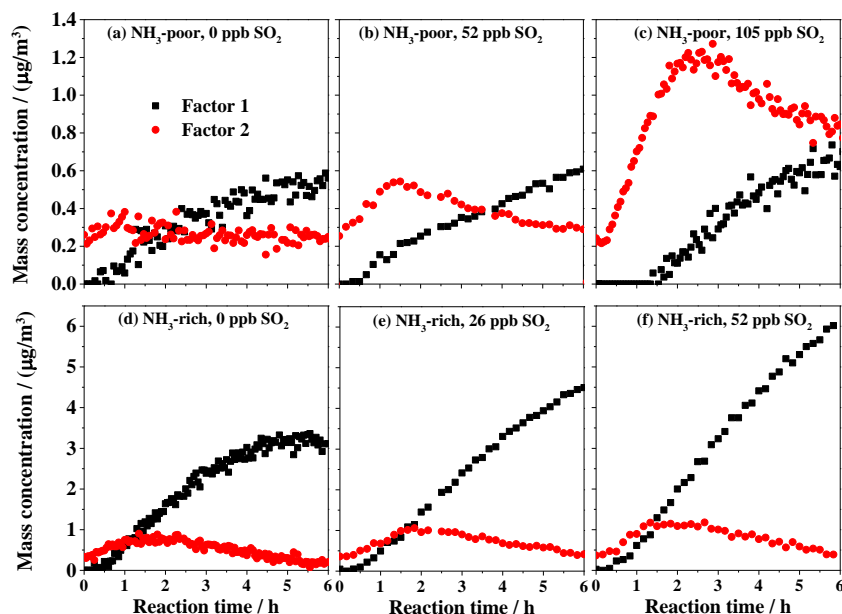
405

406 Fig. 7 The difference mass spectra (Factor 2 – Factor 1) between the two factors of
407 the generated organic aerosol identified by applying PMF analysis to the AMS
408 data

409 These two factors had different temporal variations during the reaction.
410 As indicated in Fig. 8, Factor 2 always increased at the beginning of the
411 reaction but decreased after reaching a peak with 1 or 2 hours of irradiation.
412 Factor 1 was generated later than Factor 2, while it continuously increased
413 during the reaction. Comparing experiments with different concentrations
414 of SO₂, the production of Factor 2 increased with increasing SO₂ under
415 NH₃-poor conditions, while Factor 1 increased with increasing SO₂ under
416 an NH₃-rich environment. Similar results can also be found in Fig. 9. The
417 higher production of Factor 2 with higher SO₂ under an NH₃-poor
418 environment could be probably attributed to the well-known acid-catalysis



419 effects of the oxidation product of SO₂, i.e. sulfuric acid, on heterogeneous
420 aldol condensation (Offenberg et al., 2009; Jang et al., 2002; Gao et al.,
421 2004). Under NH₃-rich conditions, however, Factor 1, which has higher
422 contents of oxygen and nitrogen than Factor 2, dominated in the SOA
423 formation. Meanwhile, the production of Factor 2 increased significantly
424 with increasing SO₂ concentration in NH₃-rich conditions. This indicated
425 that the formation of highly oxidized organic compounds and nitrogenous
426 organic compounds was increased with higher concentrations of SO₂ under
427 NH₃-rich conditions. By inference and from the results of AMS
428 measurements, aerosol water increased as the initial concentration of SO₂
429 increased, since more inorganic aerosol was generated. Liggio and Li
430 (2013) suggest that dissolution of primary polar gases into a partially
431 aqueous aerosol contributed to the increase of organic mass and oxygen
432 content on neutral and near-neutral seed aerosols, which would also take
433 place in the NH₃-rich experiments and contribute to the generation of
434 Factor 1.
435



436

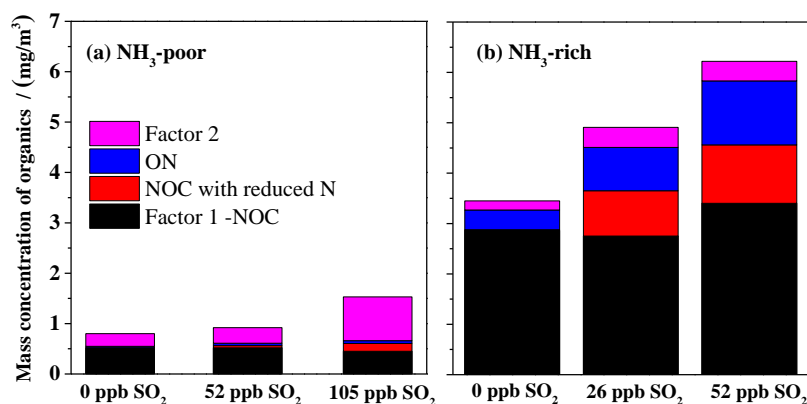
437 Fig. 8 Temporal variations of Factor 1 and Factor 2 in the presence of different

438 concentrations of SO₂ under NH₃-poor and NH₃-rich conditions.

439 Nitrogen-containing organics (NOC) are a potentially important aspect
440 of SOA formation, and may have contributed to the increase of Factor 1 in
441 this study. NOC might contain organonitrates, formed through reactions
442 between organic peroxy radicals (RO₂) and NO (Arey et al., 2001), organic
443 ammonium salts, generated in acid-base reactions between
444 ammonia/ammonium and organic acid species (Liu et al., 2012b), and
445 species with carbon covalently bonded to nitrogen, generated in reactions
446 of ammonia/ammonium with carbonyl functional group organics (Wang et
447 al., 2010). Although we were not able to measure NOC, some indirect
448 estimation methods suggested by Farmer et al. (2010) could be applied.
449 The details for estimation of the concentrations of organonitrates and NOC



450 with reduced N are given in the supporting information. Despite the
451 uncertainty, there is an obvious increasing trend of organonitrates and NOC
452 with reduced N with increasing SO_2 concentration under NH_3 -rich
453 conditions, as shown in Fig. 9. The increase ratio of NOC is higher than
454 that of the organic aerosol or Factor 1 as SO_2 concentration increases. The
455 estimated NOC contributed most of the increase in Factor 1 in NH_3 -rich
456 conditions. These results provide some evidence that the formation of
457 organonitrates and NOC with reduced N (organic ammonium salts, imines,
458 imidazole, and so on) played an important role in the increasing trend of
459 SOA with SO_2 in a NH_3 -rich environment. It was speculated that the higher
460 surface acidity of aerosol formed in the presence of a high concentration of
461 SO_2 favors NOC formation through NH_3 uptake by SOA, as observed in a
462 recent work (Liu et al., 2015b).



463

464 Fig. 9 The estimated concentrations of NOC (ON+NOC with reduced N)
465 and the two factors (identified by PMF analysis) in SOA as a function
466 of SO_2 concentration in photooxidation of toluene/ NO_x under (a)



467 NH₃-poor and (b) NH₃-rich conditions

468 **Conclusions**

469 In the photooxidation system of toluene/NO_x, the presence of SO₂
470 and/or NH₃ increased secondary aerosol formation markedly, regardless of
471 whether Al₂O₃ seed aerosol was present or not. Some synergetic effects in
472 the heterogeneous process were observed in secondary inorganic aerosol
473 formation in addition to the generation of ammonium and sulfate from NH₃
474 and SO₂. Specifically, the generation of NH₄NO₃ was found to be highly
475 dependent on the surface area concentration of suspended particles, and
476 was enhanced by increased SO₂ concentration. Meanwhile, sulfate
477 formation was also increased in the presence of NH₃. The absorbed NH₃
478 might provide liquid surface layers for the absorption and subsequent
479 reaction for SO₂ and organic products, and therefore, enhance sulfate and
480 SOA formation. NH₃ mainly influenced secondary aerosol formation in the
481 heterogeneous process, resulting in significant growth of seed aerosols, but
482 had little influence on new particle generation. In the experiments carried
483 out in the presence of Al₂O₃ seed aerosols, sulfate, organic aerosol, nitrate
484 and ammonium were all found to increase linearly with increasing SO₂
485 concentrations in toluene/NO_x photooxidation. The increase of these four
486 species was more obvious under NH₃-rich conditions, and the order of their
487 sensitivity was different from that under NH₃-poor conditions. A better
488 correlation between secondary aerosol formation and particle surface area
489 than that with particle volume indicated an enhancement effect in the



490 heterogeneous process rather than in bulk reactions.

491 Two factors were identified in the PMF analysis of the AMS data. One
492 factor assigned to less-oxidized organic aerosol and some oligomers
493 increased with increasing SO₂ under NH₃-poor conditions, mainly due to
494 the well-known acid catalytic effects of the acid products on SOA
495 formation in the heterogeneous process. The other factor, assigned to the
496 highly oxidized organic component and some nitrogenous organic
497 compounds, increased with increasing SO₂ under an NH₃-rich environment,
498 with NOC (organonitrates and NOC with reduced N) contributing most of
499 the increase.

500 This study indicated that the synergistic effects between inorganic
501 pollutants could substantially enhance secondary inorganic aerosol
502 formation. Meanwhile, the presence of inorganic gas pollutants, i.e. SO₂
503 and NH₃, promoted SOA formation markedly. Synergistic formation of
504 secondary inorganic and organic aerosol might increase the secondary
505 aerosol load in the atmosphere. These synergistic effects were related to
506 the heterogeneous process on the aerosol surface, and need to be quantified
507 and considered in air quality models.

508 **Acknowledgments**

509 This work was supported by the National Natural Science Foundation of
510 China (21407158), the “Strategic Priority Research Program” of the
511 Chinese Academy of Sciences (XDB05010300, XDB05040100,
512 XDB05010102), and the special fund of the State Key Joint Laboratory of



513 Environment Simulation and Pollution Control (14Z04ESPCR). This work
514 was also financially and technically supported by Toyota Motor
515 Corporation and Toyota Central Research and Development Laboratories
516 Inc.

517 **References**

- 518 Amarnath, V., Anthony, D. C., Amarnath, K., Valentine, W. M., Wetterau, L. A., and
519 Graham, D. G.: Intermediates in the Paal-Knorr Synthesis of Pyrroles, *J. Org. Chem.*,
520 56, 6924-6931, DOI 10.1021/jo00024a040, 1991.
- 521 Arey, J., Aschmann, S. M., Kwok, E. S. C., and Atkinson, R.: Alkyl nitrate,
522 hydroxyalkyl nitrate, and hydroxycarbonyl formation from the NO_x-air
523 photooxidations of C-5-C-8 n-alkanes, *J. Phys. Chem. A*, 105, 1020-1027, DOI
524 10.1021/jp003292z, 2001.
- 525 Bai, Y., Thompson, G. E., and Martinez-Ramirez, S.: Effects of NO₂ on oxidation
526 mechanisms of atmospheric pollutant SO₂ over Baumberger sandstone, *Building and*
527 *Environment*, 41, 486-491, DOI 10.1016/j.buildenv.2005.02.007, 2006.
- 528 Behera, S. N., and Sharma, M.: Degradation of SO₂, NO₂ and NH₃ leading to formation
529 of secondary inorganic aerosols: An environmental chamber study, *Atmos. Environ.*,
530 45, 4015-4024, DOI 10.1016/j.atmosenv.2011.04.056, 2011.
- 531 Chu, B., Hao, J., Takekawa, H., Li, J., Wang, K., and Jiang, J.: The remarkable effect
532 of FeSO₄ seed aerosols on secondary organic aerosol formation from photooxidation of
533 α -pinene/NO_x and toluene/NO_x, *Atmos. Environ.*, 55, 26-34, DOI
534 10.1016/j.atmosenv.2012.03.006, 2012.
- 535 Chu, B., Liu, Y., Li, J., Takekawa, H., Liggio, J., Li, S.-M., Jiang, J., Hao, J., and He,
536 H.: Decreasing effect and mechanism of FeSO₄ seed particles on secondary organic
537 aerosol in α -pinene photooxidation, *Environ. Pollut.*, 193, 88-93, DOI
538 [10.1016/j.envpol.2014.06.018](https://doi.org/10.1016/j.envpol.2014.06.018), 2014.
- 539 Dan, M., Zhuang, G., Li, X., Tao, H., and Zhuang, Y.: The characteristics of
540 carbonaceous species and their sources in PM_{2.5} in Beijing, *Atmos. Environ.*, 38, 3443-
541 3452, DOI [10.1016/j.atmosenv.2004.02.052](https://doi.org/10.1016/j.atmosenv.2004.02.052), 2004.
- 542 Duan, F., He, K., Ma, Y., Jia, Y., Yang, F., Lei, Y., Tanaka, S., and Okuta, T.:
543 Characteristics of carbonaceous aerosols in Beijing, China, *Chemosphere*, 60, 355-364,
544 2005.



- 545 Edney, E. O., Kleindienst, T. E., Jaoui, M., Lewandowski, M., Offenberg, J. H., Wang,
546 W., and Claeys, M.: Formation of 2-methyl tetrols and 2-methylglyceric acid in
547 secondary organic aerosol from laboratory irradiated isoprene/NO_x/SO₂/air mixtures
548 and their detection in ambient PM_{2.5} samples collected in the eastern United States,
549 *Atmos. Environ.*, 39, 5281-5289, DOI 10.1016/j.atmosenv.2005.05.031, 2005.
- 550 Farmer, D. K., Matsunaga, A., Docherty, K. S., Surratt, J. D., Seinfeld, J. H., Ziemann,
551 P. J., and Jimenez, J. L.: Response of an aerosol mass spectrometer to organonitrates
552 and organosulfates and implications for atmospheric chemistry, *Proc. Natl. Acad. Sci.*
553 *USA*, 107, 6670-6675, DOI 10.1073/pnas.0912340107, 2010.
- 554 Fu, X., Wang, S. X., Ran, L. M., Pleim, J. E., Cooter, E., Bash, J. O., Benson, V., and
555 Hao, J. M.: Estimating NH₃ emissions from agricultural fertilizer application in China
556 using the bi-directional CMAQ model coupled to an agro-ecosystem model, *Atmos.*
557 *Chem. Phys.*, 15, 6637-6649, DOI 10.5194/acp-15-6637-2015, 2015.
- 558 Gao, S., Ng, N. L., Keywood, M., Varutbangkul, V., Bahreini, R., Nenes, A., He, J. W.,
559 Yoo, K. Y., Beauchamp, J. L., Hodyss, R. P., Flagan, R. C., and Seinfeld, J. H.: Particle
560 phase acidity and oligomer formation in secondary organic aerosol, *Environ. Sci. &*
561 *Technol.*, 38, 6582-6589, DOI 10.1021/es049125k, 2004.
- 562 He, H., Wang, Y., Ma, Q., Ma, J., Chu, B., Ji, D., Tang, G., Liu, C., Zhang, H., and Hao,
563 J.: Mineral dust and NO_x promote the conversion of SO₂ to sulfate in heavy pollution
564 days, *Sci. Rep.*, 4, 04172, DOI 10.1038/srep04172, 2014.
- 565 Jang, M. S., and Kamens, R. M.: Characterization of secondary aerosol from the
566 photooxidation of toluene in the presence of NO_x and 1-propene, *Environ. Sci. &*
567 *Technol.*, 35, 3626-3639, DOI 10.1021/es010676+, 2001.
- 568 Jang, M. S., Czoschke, N. M., Lee, S., and Kamens, R. M.: Heterogeneous atmospheric
569 aerosol production by acid-catalyzed particle-phase reactions, *Science*, 298, 814-817,
570 2002.
- 571 Jaoui, M., Edney, E. O., Kleindienst, T. E., Lewandowski, M., Offenberg, J. H., Surratt,
572 J. D., and Seinfeld, J. H.: Formation of secondary organic aerosol from irradiated alpha-
573 pinene/toluene/NO_x mixtures and the effect of isoprene and sulfur dioxide, *J. Geophys.*
574 *Res.- Atmos.*, 113, D09303, DOI 10.1029/2007jd009426, 2008.
- 575 Kleindienst, T. E., Edney, E. O., Lewandowski, M., Offenberg, J. H., and Jaoui, M.:
576 Secondary organic carbon and aerosol yields from the irradiations of isoprene and
577 alpha-pinene in the presence of NO_x and SO₂, *Environ. Sci. & Technol.*, 40, 3807-3812,
578 DOI 10.1021/es052446r, 2006.
- 579 Li, W. J., Shao, L. Y., Shi, Z. B., Chen, J. M., Yang, L. X., Yuan, Q., Yan, C., Zhang, X.
580 Y., Wang, Y. Q., Sun, J. Y., Zhang, Y. M., Shen, X. J., Wang, Z. F., and Wang, W. X.:



- 581 Mixing state and hygroscopicity of dust and haze particles before leaving Asian
582 continent, *J. Geophys. Res.- Atmos.*, 119, 1044-1059, DOI 10.1002/2013jd021003,
583 2014.
- 584 Liggio, J., and Li, S. M.: Reactive uptake of pinonaldehyde on acidic aerosols, *J.*
585 *Geophys. Res.- Atmos.*, 111, DOI 10.1029/2005jd006978, 2006.
- 586 Liggio, J., Li, S. M., Brook, J. R., and Mihele, C.: Direct polymerization of isoprene
587 and alpha-pinene on acidic aerosols, *Geophysical Research Letters*, 34, DOI
588 10.1029/2006gl028468, 2007.
- 589 Liggio, J., and Li, S. M.: Reversible and irreversible processing of biogenic olefins on
590 acidic aerosols, *Atmos. Chem. Phys.*, 8, 2039-2055, 2008.
- 591 Liggio, J., and Li, S. M.: A new source of oxygenated organic aerosol and oligomers,
592 *Atmos. Chem. Phys.*, 13, 2989-3002, DOI 10.5194/acp-13-2989-2013, 2013.
- 593 Lin, Y. H., Knipping, E. M., Edgerton, E. S., Shaw, S. L., and Surratt, J. D.:
594 Investigating the influences of SO₂ and NH₃ levels on isoprene-derived secondary
595 organic aerosol formation using conditional sampling approaches, *Atmos. Chem. Phys.*,
596 13, 8457-8470, DOI 10.5194/acp-13-8457-2013, 2013.
- 597 Liu, C., Liu, Y., Ma, Q., and He, H.: Mesoporous transition alumina with uniform pore
598 structure synthesized by alumisol spray pyrolysis, *Chem. Eng. J.*, 2010.
- 599 Liu, C., Ma, Q., Liu, Y., Ma, J., and He, H.: Synergistic reaction between SO₂ and NO₂
600 on mineral oxides: a potential formation pathway of sulfate aerosol, *Phys. Chem. Chem.*
601 *Phys.*, 14, 1668-1676, DOI 10.1039/c1cp22217a, 2012a.
- 602 Liu, X. G., Li, J., Qu, Y., Han, T., Hou, L., Gu, J., Chen, C., Yang, Y., Liu, X., Yang, T.,
603 Zhang, Y., Tian, H., and Hu, M.: Formation and evolution mechanism of regional haze:
604 a case study in the megacity Beijing, China, *Atmos. Chem. Phys.*, 13, 4501-4514, DOI
605 10.5194/acp-13-4501-2013, 2013.
- 606 Liu, X. G., Sun, K., Qu, Y., Hu, M., Sun, Y. L., Zhang, F., and Zhang, Y. H.: Secondary
607 Formation of Sulfate and Nitrate during a Haze Episode in Megacity Beijing, China,
608 *Aerosol Air Qual. Res.*, 15, 2246-2257, DOI 10.4209/aaqr.2014.12.0321, 2015a.
- 609 Liu, Y., Ma, Q., and He, H.: Heterogeneous Uptake of Amines by Citric Acid and
610 Humic Acid, *Environ. Sci. & Technol.*, 46, 11112-11118, 10.1021/es302414v, 2012b.
- 611 Liu, Y., Liggio, J., Staebler, R., and Li, S. M.: Reactive uptake of ammonia to secondary
612 organic aerosols: kinetics of organonitrogen formation, *Atmos. Chem. Phys.*, 15,
613 13569-13584, DOI 10.5194/acp-15-13569-2015, 2015b.
- 614 Meng, Z., Xie, Y., Jia, S., Zhang, R., Lin, W., Xu, X., and Yang, W.: Characteristics of
615 Atmospheric Ammonia at Gucheng, a Rural Site on North China Plain in Summer of
616 2013, *J. Appl. Meteor. Sci.*, 26, 141-150, 2015.



- 617 Meyer, N. K., Duplissy, J., Gysel, M., Metzger, A., Dommen, J., Weingartner, E.,
618 Alfarra, M. R., Prevot, A. S. H., Fletcher, C., Good, N., McFiggans, G., Jonsson, A. M.,
619 Hallquist, M., Baltensperger, U., and Ristovski, Z. D.: Analysis of the hygroscopic and
620 volatile properties of ammonium sulphate seeded and unseeded SOA particles, Atmos.
621 Chem. Phys., 9, 721-732, 2009.
- 622 Na, K., Song, C., and Cocker, D. R.: Formation of secondary organic aerosol from the
623 reaction of styrene with ozone in the presence and absence of ammonia and water,
624 Atmos. Environ., 40, 1889-1900, DOI 10.1016/j.atmosenv.2005.10.063, 2006.
- 625 Na, K., Song, C., Switzer, C., and Cocker, D. R.: Effect of ammonia on secondary
626 organic aerosol formation from alpha-Pinene ozonolysis in dry and humid conditions,
627 Environ. Sci. & Technol., 41, 6096-6102, DOI 10.1021/es061956y, 2007.
- 628 Ng, N. L., Herndon, S. C., Trimborn, A., Canagaratna, M. R., Croteau, P. L., Onasch,
629 T. B., Sueper, D., Worsnop, D. R., Zhang, Q., Sun, Y. L., and Jayne, J. T.: An Aerosol
630 Chemical Speciation Monitor (ACSM) for routine monitoring of the composition and
631 mass concentrations of ambient aerosol, Aerosol Sci. Technol., 45, 770-784, DOI
632 10.1080/02786826.2011.560211, 2011.
- 633 Offenberg, J. H., Lewandowski, M., Edney, E. O., Kleindienst, T. E., and Jaoui, M.:
634 Influence of Aerosol Acidity on the Formation of Secondary Organic Aerosol from
635 Biogenic Precursor Hydrocarbons, Environ. Sci. & Technol., 43, 7742-7747, DOI
636 10.1021/es901538e, 2009.
- 637 Pathak, R. K., Wu, W. S., and Wang, T.: Summertime PM_{2.5} ionic species in four major
638 cities of China: nitrate formation in an ammonia-deficient atmosphere, Atmos. Chem.
639 Phys., 9, 1711-1722, 2009.
- 640 Santiago, M., Garcia Vivanco, M., and Stein, A. F.: SO₂ effect on secondary organic
641 aerosol from a mixture of anthropogenic VOCs: experimental and modelled results,
642 International Journal of Environment and Pollution, 50, 224-233, 2012.
- 643 Schmitt-Kopplin, P., Gelencser, A., Dabek-Zlotorzynska, E., Kiss, G., Hertkorn, N.,
644 Harir, M., Hong, Y., and Gebefuegi, I.: Analysis of the Unresolved Organic Fraction in
645 Atmospheric Aerosols with Ultrahigh-Resolution Mass Spectrometry and Nuclear
646 Magnetic Resonance Spectroscopy: Organosulfates As Photochemical Smog
647 Constituents, Anal. Chem., 82, 8017-8026, DOI 10.1021/ac101444r, 2010.
- 648 Takekawa, H., Minoura, H., and Yamazaki, S.: Temperature dependence of secondary
649 organic aerosol formation by photo-oxidation of hydrocarbons, Atmos. Environ., 37,
650 3413-3424, DOI 10.1016/s1352-2310(03)00359-5, 2003.
- 651 Tursic, J., and Grgic, I.: Influence of NO₂ on S(IV) oxidation in aqueous suspensions
652 of aerosol particles from two different origins, Atmos. Environ., 35, 3897-3904, DOI



- 653 10.1016/s1352-2310(01)00142-x, 2001.
- 654 Tursic, J., Berner, A., Podkrajsek, B., and Grgic, I.: Influence of ammonia on sulfate
655 formation under haze conditions, *Atmos. Environ.*, 38, 2789-2795, DOI
656 10.1016/j.atmosenv.2004.02.036, 2004.
- 657 Updyke, K. M., Nguyen, T. B., and Nizkorodov, S. A.: Formation of brown carbon via
658 reactions of ammonia with secondary organic aerosols from biogenic and
659 anthropogenic precursors, *Atmos. Environ.*, 63, 22-31, DOI
660 10.1016/j.atmosenv.2012.09.012, 2012.
- 661 Wang, L., Wen, L., Xu, C., Chen, J., Wang, X., Yang, L., Wang, W., Yang, X., Sui, X.,
662 Yao, L., and Zhang, Q.: HONO and its potential source particulate nitrite at an urban
663 site in North China during the cold season, *Sci. Total Environ.*, 538, 93-101, DOI
664 [10.1016/j.scitotenv.2015.08.032](https://doi.org/10.1016/j.scitotenv.2015.08.032), 2015.
- 665 Wang, X. F., Gao, S., Yang, X., Chen, H., Chen, J. M., Zhuang, G. S., Surratt, J. D.,
666 Chan, M. N., and Seinfeld, J. H.: Evidence for High Molecular Weight Nitrogen-
667 Containing Organic Salts in Urban Aerosols, *Environ. Sci. & Technol.*, 44, 4441-4446,
668 DOI 10.1021/es1001117, 2010.
- 669 Wang, Z., Wang, T., Guo, J., Gao, R., Xue, L. K., Zhang, J. M., Zhou, Y., Zhou, X. H.,
670 Zhang, Q. Z., and Wang, W. X.: Formation of secondary organic carbon and cloud
671 impact on carbonaceous aerosols at Mount Tai, North China, *Atmos. Environ.*, 46, 516-
672 527, DOI 10.1016/j.atmosenv.2011.08.019, 2012.
- 673 Wen, L. A., Chen, J. M., Yang, L. X., Wang, X. F., Xu, C. H., Sui, X. A., Yao, L., Zhu,
674 Y. H., Zhang, J. M., Zhu, T., and Wang, W. X.: Enhanced formation of fine particulate
675 nitrate at a rural site on the North China Plain in summer: The important roles of
676 ammonia and ozone, *Atmos. Environ.*, 101, 294-302, DOI
677 10.1016/j.atmosenv.2014.11.037, 2015.
- 678 Wu, S., Lu, Z. F., Hao, J. M., Zhao, Z., Li, J. H., Hideto, T., Hiroaki, M., and Akio, Y.:
679 Construction and characterization of an atmospheric simulation smog chamber,
680 *Advances in Atmospheric Sciences*, 24, 250-258, DOI 10.1007/s00376-007-0250-3,
681 2007.
- 682 Yang, F., Tan, J., Zhao, Q., Du, Z., He, K., Ma, Y., Duan, F., Chen, G., and Zhao, Q.:
683 Characteristics of PM_{2.5} speciation in representative megacities and across China,
684 *Atmos. Chem. Phys.*, 11, 5207-5219, DOI 10.5194/acp-11-5207-2011, 2011.
- 685 Yang, W., He, H., Ma, Q., Ma, J., Liu, Y., Liu, P., and Mu, Y.: Synergistic formation of
686 sulfate and ammonium resulting from reaction between SO₂ and NH₃ on typical mineral
687 dust, *Phys. Chem. Chem. Phys.*, 18, 956-964, DOI 10.1039/c5cp06144j, 2016.
- 688 Ye, X. N., Ma, Z., Zhang, J. C., Du, H. H., Chen, J. M., Chen, H., Yang, X., Gao, W.,



689 and Geng, F. H.: Important role of ammonia on haze formation in Shanghai, Environ.
690 Res. Lett., 6, Artn 024019, DOI 10.1088/1748-9326/6/2/024019, 2011.

691 Zhao, P. S., Dong, F., He, D., Zhao, X. J., Zhang, X. L., Zhang, W. Z., Yao, Q., and Liu,
692 H. Y.: Characteristics of concentrations and chemical compositions for PM_{2.5} in the
693 region of Beijing, Tianjin, and Hebei, China, Atmos. Chem. Phys., 13, 4631-4644, DOI
694 10.5194/acp-13-4631-2013, 2013.

695 Zou, Y., Deng, X. J., Zhu, D., Gong, D. C., Wang, H., Li, F., Tan, H. B., Deng, T., Mai,
696 B. R., Liu, X. T., and Wang, B. G.: Characteristics of 1 year of observational data of
697 VOCs, NO_x and O₃ at a suburban site in Guangzhou, China, Atmos. Chem. Phys., 15,
698 6625-6636, DOI 10.5194/acp-15-6625-2015, 2015.

699